Bioorganic Chemistry 91 (2019) 103144

Contents lists available at ScienceDirect

Bioorganic Chemistry

journal homepage: www.elsevier.com/locate/bioorg

Lysosome imaging in cancer cells by pyrene-benzothiazolium dyes: An alternative imaging approach for LAMP-1 expression based visualization methods to avoid background interference

Chathura S. Abeywickrama[a,1], Kaveesha J. Wijesinghe[c,1], Robert V. Stahelin[d,*], Yi Pang[a,b,*]

[a] Department of Chemistry, University of Akron, Akron, OH 44325, USA
[b] Maurice Morton Institute of Polymer Science, University of Akron, Akron, OH 44325, USA
[c] Department of Chemistry and Biochemistry, University of Notre Dame, Notre Dame, IN 46556, USA
[d] Department of Medicinal Chemistry and Molecular Pharmacology and the Purdue Center for Cancer Research, Purdue University, West Lafayette, IN 47907, USA

ABSTRACT

A series of pyrene-benzothiazolium dyes (**1a–1d**) were experimentally investigated to study their internalization mechanism into cellular lysosomes as well as their potential imaging applications for live cell imaging. The lysosome selectivity of the probes was further compared by using fluorescently tagged lysosome associated membrane protein-1 (LAMP-1) expression-dependent visualization in both normal (COS-7, HEK293) and cancer (A549, Huh 7.5) cell lines. These probes were successfully employed as reliable lysosome markers in tumor cell models, thus providing an attractive alternative to LAMP-1 expression-dependent visualization methods. One advantage of these probes is the elimination of significant background fluorescence arising from fluorescently tagged protein expression on the cell surface when cells were transfected with LAMP-1 expression plasmids. Probes exhibited remarkable ability to stain cellular lysosomes for long-term experiments (up to 24 h) and the highly lipophilic nature of the probe design allowed their accumulation in hydrophobic regions of the cellular lysosomes. Experimental evidences indicated that the probes are likely to be internalized into lysosomes via endocytosis and accumulated in the hydrophobic regions of the lysosomes rather than in the acidic lysosomal lumen. These probes also demonstrated significant stability and lysosome staining for fixed cell imaging applications as well. Lastly, the benzothiazolium moiety of the probes was identified as the key component for lysosome selectivity.

1. Introduction

Lysosomes play critical roles in many cellular processes such as endocytosis, cellular metabolism, cell division, signal transduction, homeostasis, and autophagy [1,2]. Lysosomal digestive enzymes (hydrolases) exhibit their optimal activity in the acidic environment of the lysosomal lumen (pH 4.5–5) [3]. Lysosome dysfunction is attributed to many severe disease conditions such as neurodegenerative disorders, lysosome storage diseases, cancer and inflammations [4–10]. Lysosomal hydrolases are also known to participate in tumor growth, migration and invasion [3,11–17]. Therefore, imaging lysosomes in live or fixed cell samples has recently received much attention. For instance, correlation between lysosomal malfunction and cancer susceptibility has attracted significant attention, as recent findings show that lysosomal function could be responsible for pro-oncogenic stages [3,18]. Lysosomes are possible target organelles for cancer therapy due to their role in cross talk between apoptosis and autophagy [18–20]. Visualization of lysosomes in cancer cells is thus important in understanding lysosomal distribution, morphological changes, lysosomal pH, subcellular drug targeting and cell proliferation. Since lysosome imaging by LysoTracker® probes is not suitable for long term visualization experiments (due to “alkalinizing effect”), many studies use the expression of fluorescently tagged lysosome-associated membrane protein-1 (LAMP-1), as an alternative method to visualize lysosomes for long-term imaging purposes. This method is based on transfection of cells with fluorescently tagged lysosome specific membrane proteins that have high abundance within lysosome membranes [12,21–24]. LAMP-1 is mainly located in the endosomal-lysosomal membrane [22]. In addition, LAMP-1 is also found in other cellular membranes of healthy cells with lower abundancy (> 2%) [25]. However, in highly metastatic tumor cells (i.e., metastatic colon cancer cells), LAMP-1 expression is found to be non-specific and relatively higher levels have been observed on the cell surface membranes [25–28] Therefore, LAMP-1 expression-based methods could be of limited application for visualizing and identifying cellular lysosomes in such cancer cells due to their non-specific staining. In addition, fluorescently tagged LAMP-1 exhibits a

* Corresponding authors at: Department of Chemistry, University of Akron, Akron, OH 44325, USA (Y. Pang) and Department of Medicinal Chemistry and Molecular Pharmacology and the Purdue Center for Cancer Research, Purdue University, West Lafayette, IN 47907, USA (Robert V. Stahelin)
E-mail addresses: rstaheli@purdue.edu (R.V. Stahelin), yp5@uakron.edu (Y. Pang).
[1] Authors equally contributed.

https://doi.org/10.1016/j.bioorg.2019.103144
Received 30 May 2019; Received in revised form 3 July 2019; Accepted 19 July 2019
Available online 24 July 2019

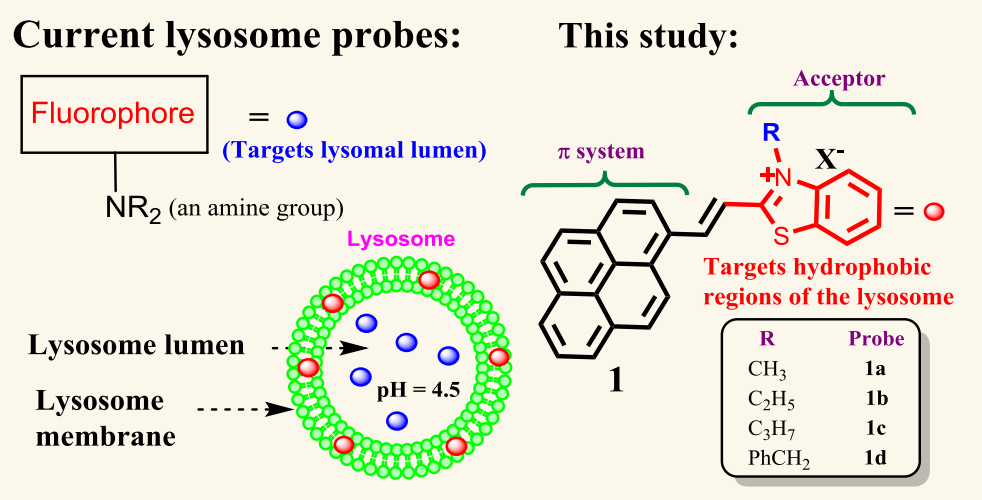

Scheme 1. Brief comparison of current lysosome probes designs vs pyrene-based probes **1**.

very narrow Stokes shift (e.g., λ_{ex} = 488 nm, λ_{em} = 510 nm, for Lysosome-GFP), requires a long expression time (~12–16 h), and has potential perturbation to structural integrity of the lysosomal membrane upon overexpression.

As an alternative approach to visualize cellular lysosomes, many chemical probes have been developed to date. Most lysosome probe designs incorporate a basic amino group as the lysosome targeting moiety (Scheme 1) such as in commercial LysoTracker® and LysoSensor® probes [29]. However, these probes require an acidic media to operate, and their accumulation in the lysosomal lumen will eventually increase lysosomal pH (i.e., "the alkalinizing effect") and perturbs cellular activities and increases cell death [30–33]. Structurally improved non-alkalinizing probe designs have been developed recently by incorporating spirolactams[34] and peptide[35] based skeletons which are inert to the acidic nature of the lysosomal lumen. In addition, existing commercial lysosome probes typically exhibit a small Stokes' shift (e.g., < 20 nm) which is a common drawback for fluorescent microscopy-based applications. In order to meet the increased demand for lysosome sensing, there are significant interests in the field for developing novel probes with emission in near infrared (NIR) region, [31,36–38], and new probes for real-time tracking of lysosomes [1,31,39–41].

In order to overcome the challenges associated with the existing lysosome visualization methods mentioned above, it is desirable to develop novel highly selective and biocompatible lysosome probes, whose fluorescence activation does not require acidic environment and whose structural features do not contain basic functional groups. Such probes could open the possibility for long-term imaging of lysosomal distribution, which is essential for screening lysosomes in cancer cells. We have recently reported the pyrene-based fluorescent probes **1a–1d** that exhibit remarkable selectivity to cellular lysosomes, giving bright red fluorescence turn on upon lysosomal localization [42]. Since the probe series **1** does not incorporate any basic functional groups (Scheme 1), it could be used to track cellular lysosome activities for longer durations without "alkalinizing effect." Also, our further research illustrated that probes **1a** − **1d** appear to function by localizing into the hydrophobic regions of the lysosome (i.e., membrane), rather than in the acidic lysosomal lumen, thereby avoiding potential perturbation to lysosome activities. The study indicated that these pyrene-based probes could be successfully employed as an alternative imaging tool for visualizing lysosomes in cancer cells by avoiding background interference arising from LAMP-1 expression based visualizing methods as well as cytotoxicity that occurs with commercial Lysotracker® probes due to the alkalinizing effect.

2. Materials and methods

All chemicals for synthesis were purchased from Sigma-Aldrich and Fisher Scientific. All molecular biology grade reagents for cell culture and fluorescent confocal microscopy were purchased from Sigma-Aldrich, Fisher scientific, Abcam or Addgene. UV–vis studies were carried out in a Hewlett Packard-8453 diode array spectrophotometer at 25 °C. Fluorescence studies were carried out using a HORIBA Fluoromax-4 spectrofluorometer. Fluorescence confocal images were obtained from a Zeiss LSM 710 confocal microscope. Cell viability assays were carried out by using a Spectramax® M5e multimode microplate reader. *Cercopithecus aethiops* (African green monkey kidney cells) Kidney cells (COS-7), Adeno-carcinomic human alveolar basal epithelial cells (A549), and Human hepatocyte-derived carcinoma cells (Huh 7.5) were used for cell studies.

2.1. Cell culture and transfection

COS-7 and HEK293 cells were maintained in Dulbecco's modified Eagle's medium (DMEM) (Invitrogen) containing 1% FBS and 1% Penstrep at 37 °C in a 5% CO_2 humidified incubator. A549 and Huh 7.5 cells were maintained in Roswell Park Memorial Institute (RPMI) medium (Invitrogen) containing 1% FBS and 1% Penstrep at 37 °C in a 5% CO_2 humidified incubator. The cells were grown to 70–80% confluency before passage or transfection. Live cell imaging plates were prepared by plating cells in MatTek chambered cell culture plates. Transfections were performed using Lipofectamine 2000 reagent according to the manufacturer's protocol. mTurquoise Lysosome-20 transfected cells were incubated for 14 h and CellLight Lysosome-GFP treated cells were incubated for a 12-h period.

2.2. Cell treatments with fluorescent probes

Probes **1a–1d**, LysoTracker® Green DND-26 solutions were made in DMSO. For live cell imaging, cells were treated with 100–500 nM probes **1a–1d** (final concentration) in PBS for 30 min at 37 °C. During co-localization studies, cells were treated with 70 nM LysoTracker® Green DND-26. Final DMSO percentage in cell media was < 0.25% (V/V). For initial cell studies, cells were treated with probes (**1a–1d**) for fluorescent confocal imaging without further washing. During co-localization studies with LysoTracker® probes, cells were washed 3 times with 1 × PBS.

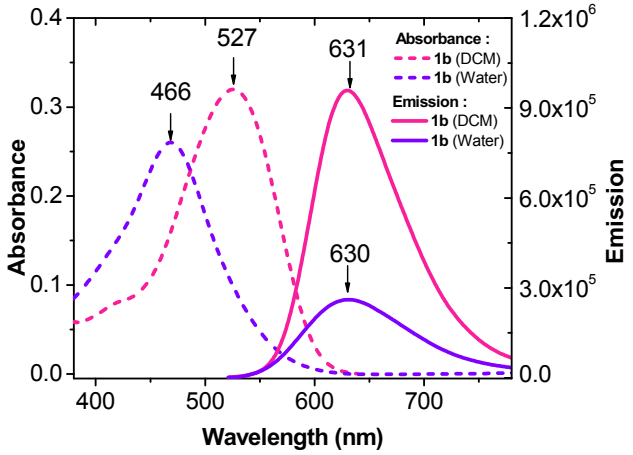

Fig. 1. Absorbance and emission spectra of **1b** (1×10^{-5} M) in different solvents at room temperature. Probes were excited at 500 nm to obtain emission spectra.

2.3. Fluorescence confocal microscopy

Cells were imaged using a Zeiss LSM 710 fluorescence confocal microscope with an oil 63× 1.4 numerical aperture objective. For the nuclear co-localization experiments, mTurquoise-H2A-10 and mTurquoise Lysosome-20 (kind gifts from Dr. Michael Davidson, Addgene plasmid #55556 and 55568, respectively) transfected cells were excited with a 454 nm laser line and emission was collected from 465 nm to 530 nm range. CellLight Lysosome-GFP, and LysoTracker® Green DND-26 were excited with a 488 nm laser and emission was collected from 500 nm to 580 nm range. Probes **1a–1d** were excited with 561 nm laser and emission was collected from 585 nm to 700 nm range. Co-localization experiment results were further analyzed using the Zeiss LSM software and Mander's overlap coefficient was calculated by ImageJ (NIH) software. Mander's overlap coefficient values greater than 0.6 confirms an acceptable significant co-localization of the two fluorophores. For fixed cell imaging, pm Turquoise2- H2A transfected cells were first fixed by incubating in ice cold 100% methanol at −20 °C for 15 min. Following cell fixation, cells were washed three times with PBS for 5 min each and treated with probe 1 (500 nM) for 1 h at 37 °C.

2.4. Log P value determination

Log P values were calculated according to the previously reported method using 1-octanol (organic) and water (aqueous) at 20 °C [43,44]. Solid samples of probes **1a–1d** were initially dissolved in 1-octanol and then equilibrated in between organic and aqueous phases by using a vigorous shaking method. Partition coefficient (p) for the probe was given by following equation.

$$P = [Probe(organic)]/[Probe(aqueous)]$$

Therefore, the lipophilicity value (log P) is calculated by following equation.

$$Log\ \ P = \log_{10}\{[Probe(organic)]/[Probe(aqueous)\}$$

2.5. Spectrometric titration with protein samples

Recombinant lysosomal membrane proteins LAMP-1 (OPCD04833) and LAMP-2 (OPCD04837) protein samples were purchased from AVIVA Systems Biology and samples were used as received without further purification 5% (w/v) protein stock samples were prepared by dissolving 20 mM Tris, 150 mM NaCl (pH = 8.0) according to the manufacturer protocol. HAS samples were purchased from Sigma Aldrich and samples were used as received without further purification. 5% HSA solution was prepared by dissolving HSA sample in PBS buffer (PH 7.40). 1 mM stock solutions for probes were prepared in DMSO. All spectrometric titrations were carried out in PBS buffer (pH = 7.4) at room temperature by using quartz cuvettes. Aqueous acidic solutions (pH 4.5) for Spectrometric analysis was prepared by using 1 M HCl solution. For spectrometric titrations, protein solutions were added in 5 min. Samples were mixed gently for 1–2 min before obtaining spectroscopic data at different time intervals.

2.6. Application of endocytosis inhibitors

COS-7 cells were plated in MatTek chambered cell culture plates with Dulbecco's modified Eagle's medium (DMEM) (Invitrogen) containing 1% FBS and 1% Penstrep at 37 °C in a 5% CO_2 humidified incubator. Dynasore® and Pitstop®2 stock solutions were prepared in DMSO. Working concentrations for endocytosis inhibitors were chosen according to the manufacturer's recommendations. COS-7 cells were washed with 1x PBS for 3 times and treated with 80 μM Dynasore® in PBS for 30 min and then cells were further incubated with probes **1b** and **1d** for 30 min at 37° C. A control experiment was carried out for probes **1b** and **1d** where COS-7 cells were incubated with 500 nM probes **1b** and **1d** for 30 min prior to confocal microscope imaging. Similarly, COS-7 cells were treated with 32 μM Pitstop®2 ® in PBS for 10 min and then cells were further incubated with probes **1b** and **1d** for 30 min at 37° C. Fluorescence confocal microscopy images were obtained by exciting probes with 561 nm laser and emission was collected from 585 nm to 700 nm.

3. Results and discussion

3.1. Photophysical importance

Photophysical properties of probe **1** are summarized in Fig. 1 and ESI Table S1. Probes **1a–1d** exhibited bright red emission in the range $\lambda_{em} \sim 630$ nm–640 nm ($\phi_{fl} \approx 0.15$–0.48) in organic solvents (Fig. 1) [42]. The emission of **1** was not affected by the solvent polarity, which is a distinct advantage associated with the rigid chromophore structure. The observed large Stokes' shift ($\Delta\lambda \approx 140$ nm, 71,428 cm^{-1}) is attributed to the strong intra-molecular charge transfer (ICT) that occurs in the structure (ESI Fig. S2.1). In addition, the absorbance or emission of **1** did not show any noticeable changes in different pH environments (pH = 3–10) (ESI Fig. S2.2) [42]. Interestingly, fluorescent quantum yield of **1** was significantly lower in an aqueous environment (ESI Table S1) than that in non-polar solvents, making probe **1** suitable for cell staining under "wash-free" conditions where no post staining washing step is required prior to imaging [45]. Another potential advantage of these probes is their characteristic excitation wavelength $\lambda_{em} \approx 527$ nm, which is close to the commercially available laser lines (514 nm, 561 nm) in microscope systems for facile excitation.

3.2. Biological cell studies and imaging

The consistency of the lysosome selectivity of probe **1** was further confirmed by following different co-localization experiments in COS-7 (*Cercopithecus aethiops*) cells by using different colocalization methods. A sample of COS-7 cells were treated with CellLight® Lysosome-GFP, BacMam 2.0 for 10 h and colocalization experiments were carried out by incubating the transfected cells with **1b** (500 nM) for 30 min (Fig. 2, ESI Fig. S3). Alternatively, COS-7 cells were also transfected with mTurquoise-Lysosomes-20 for 12 h[46] and then cells were stained with **1b** or **1d** (500 nM) for 30 min (Fig. 2). Both colocalization experiments exhibited calculated Mander's overlap coefficient > 0.92 confirming exceptional lysosome selectivity of probe **1**. As a control experiment, non-transfected COS-7 cells were co-stained with LysoTracker® Green DND-26 (70 nM) and probe **1** (500 nM) for 30 min (Fig. 3, ESI Fig. S4) and produced excellent colocalization results (calculated Mander's overlap coefficient > 0.90). Further colocalization experiments were conducted for probe **1** in HEK293 (Human embryonic

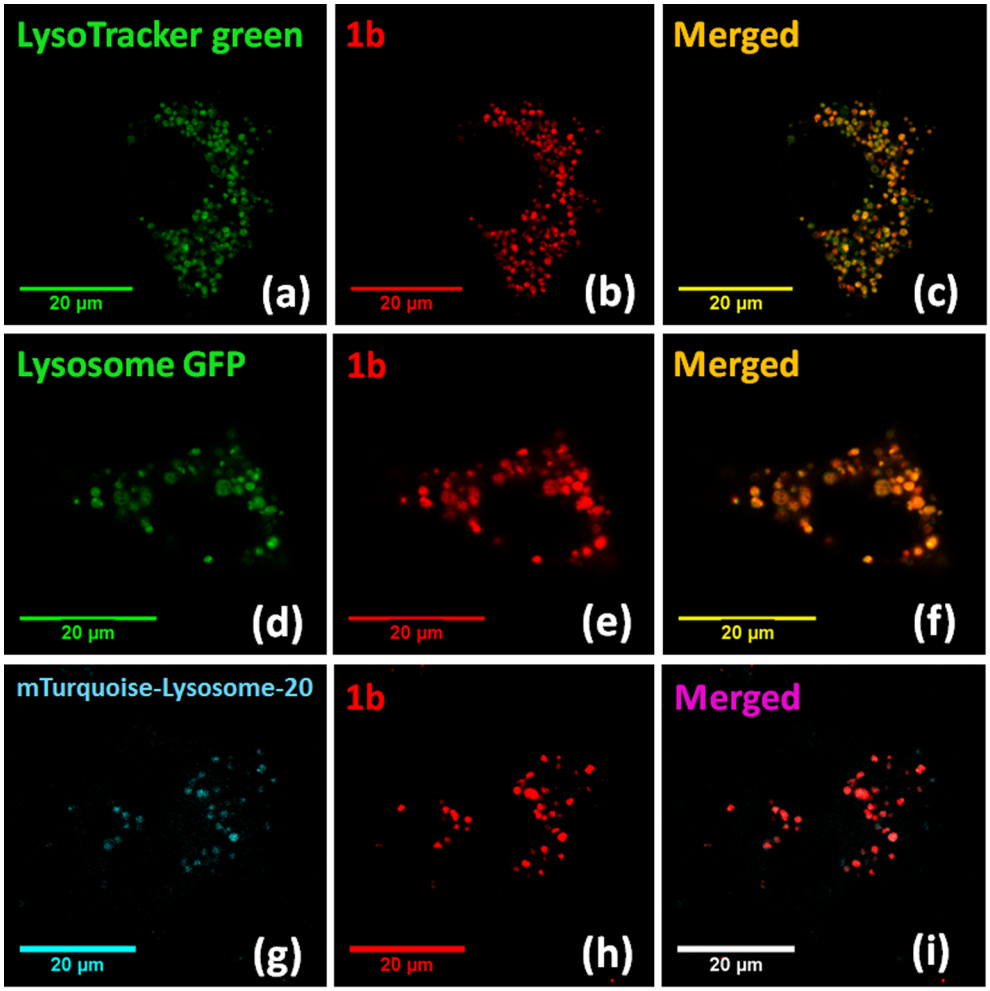

Fig. 2. Fluorescence confocal microscopy images of COS-7 cells incubated with probe **1b** (500 nM) for 30 min under different co-localization methods. Images a – i represents LysoTracker® Green DND-26 (70 nm, a), probe **1b** (b,e,h), CellLight® lysosome-GFP expression (d), mTuquoise-Lysosome-20 expression (g) and respective overlapped images (c,f,i). Probe **1b** was excited with a 561 nm laser and Lysotracker® Green and CellLight® Lysosome-GFP were excited with a 488 nm laser line. mTurquoise-Lysosome-20 expression was visualized by a 454 nm laser. All images were obtained at 63× oil magnification.

kidney cells 293) cells (ESI Fig. S5). This experimental result thus further verified that probe **1** is a reliable lysosome-targeting probe, despite its simplicity in use.

The remarkable lysosome selectivity observed from the normal cell lines (Fig. 2, ESI Fig. S3-4) encouraged us to further examine the probe's application on cancer cell lines. CellLight® Lysosome-GFP was expressed (8–10 h) in A549 (Adeno-carcinomic human alveolar basal epithelial cells) and Huh 7.5 (Human hepatocyte-derived carcinoma cell) cells for for colocalization experiments with **1**. However, CellLight® Lysosme-GFP expression in these cell lines showed a significant background due to non-specific expression of the fluorescence protein (LAMP-1) throughout the cell (Fig. 3). The observations were further confirmed by repeated LAMP-1 expression-based imaging experiments. In contrast, CellLight® Lysosome-GFP expression carried out in healthy cells (COS-7) did not show any noticeable background from the protein expression (Fig. 2).

In contrast, A549 cells co-stained with commercial LysoTacker® Red DND-99 and probe **1** (500 nM) produced excellent co-localization patterns (Calculated mander's overlap coefficient > 0.9) (ESI Fig. S6-7). Transfection based lysosome screening methods such as CellLight® Lysosome-GFP and mTurquoise-Lysosome-20 are most frequently used reliable methods for visualizing lysosomes for long term imaging purposes, due to their non-toxic and high level of cell compatibility. These methods are based on expressing fluorescently tagged lysosome associated membrane protein-1 (LAMP-1) which is highly abundant in lysosomes. However, in highly metastatic cancer cells, LAMP-1 expression is found to be not specific for cellular lysosomes where expression of LAMP-1 also occurs in cell membranes as well as on cell surface [12]. Therefore, visualization of lysosomes via LAMP-1 expression based methods can be questionable for identifying lysosomes due to non-specific visualization patterns in cancer cells. This is a major challenging situation in transfection-based methodologies for screening lysosomes in tumor cells by LAMP-1 expression dependent techniques. Due to the potential alkalinizing effect, commercial LysoTracker® probes are not recommended for long term imaging experiments. Interestingly, the new pyrene-based probe series (**1a–1d**) could be an exceptionally useful tool under this situation for visualizing lysosome in cancer cells for disease related study purposes.

Cell viability studies for probes were previously conducted by CellTiter-Glow® Luminescencent cell viability assays and experimental LC_{50} values obtained for the probe series were found to be in the 25–30 μM range [42]. The observed lower toxicity further confirmed that these probes are suitable for biological cell studies where the working concentration of the probes were significantly lower than their LC_{50} value. Probe **1** was further studied in the presence of different fluorescent proteins expressed in A549 cells such as GFP-C1-PLCδ-PH (plasma membrane) and mTurquoise-H2A-10 (nucleus) to confirm their suitability to use with different protein expression-based methods without interferences (Fig. 4). Interestingly, visualization of cellular lysosomes in these transfected cells was very clear and probe **1**

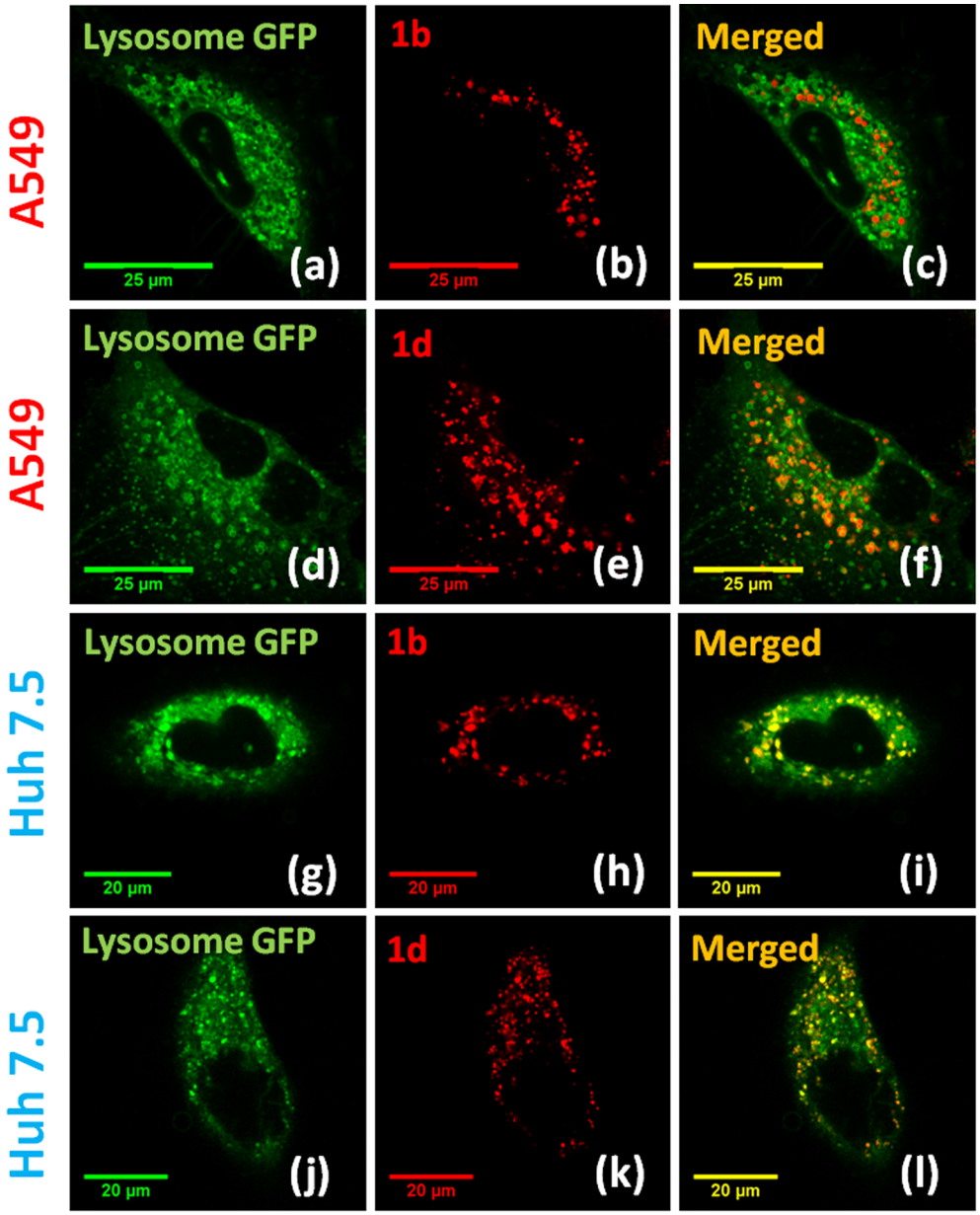

Fig. 3. Fluorescence confocal microscopy images of CellLight® Lysosome-GFP transfected A549 and Huh 7.5 cells incubated for 30 min with probe **1b** and **1d** (500 nM). Images a,d,h and j shows fluorescence microscope images of CellLight®Lysosome-GFP expression, images b and h represents images of probe **1b** and Images e and k represents images of probe **1d**. Images c,f,I, and l represents overlapped figures for **1b** (c,i) and **1d** (f,l)with Lysosome-GFP. Probe **1b** and **1d** were excited with a 561 nm laser and Lysosome-GFP was excited with 488 nm laser line. All images were obtained at 63× oil magnification.

produced excellent bright red confocal images without any interferences. Therefore, pyrene-based probes **1** will be a reliable tool for staining lysosomes in differently transfected cells for a variety of biological applications.

3.3. Fixed cell imaging ability

Excellent imaging ability observed in live cell samples encouraged us to investigate the ability of probe **1** to stain fixed cells. A549 cells were first fixed by a methanol-based cell fixation method and then incubated with **1b** (500 nM) for 30 min. Fixed cell samples were analyzed by fluorescent confocal microscopy. In fixed cell samples, probe **1b** generated bright red fluorescence confirming its ability to stain fixed cells (Fig. 5). Alternatively, A549 cells were first incubated with probe **1b** (500 nM) for 30 min and then fixed with methanol (ESI Fig. S9). Interestingly, both prior and post fixation cell staining with probe **1b** produced excellent confocal microscopy images, indicating its flexibility in fixed cell experiments. It is also important to note that many live cell imaging fluorescent probes are not compatible for fixed cell experiments. Therefore, probe **1** could be a potentially useful tool for many biological aspects as cell fixation is essential for many important studies.

3.4. Long-term imaging ability

Long-term imaging ability of probe **1** was examined by obtaining fluorescent confocal microscopy images of A549 cells treated with **1b** (500 nM) for a 1–24-h period (Fig. 6). Surprisingly, probe **1b** produced a consistent bright red emission pattern up to 24 h proving its highly biocompatible nature and stability to employ in long-term imaging experiments. Also, it is important to note that cells did not show any observable morphological changes. In control experiments we

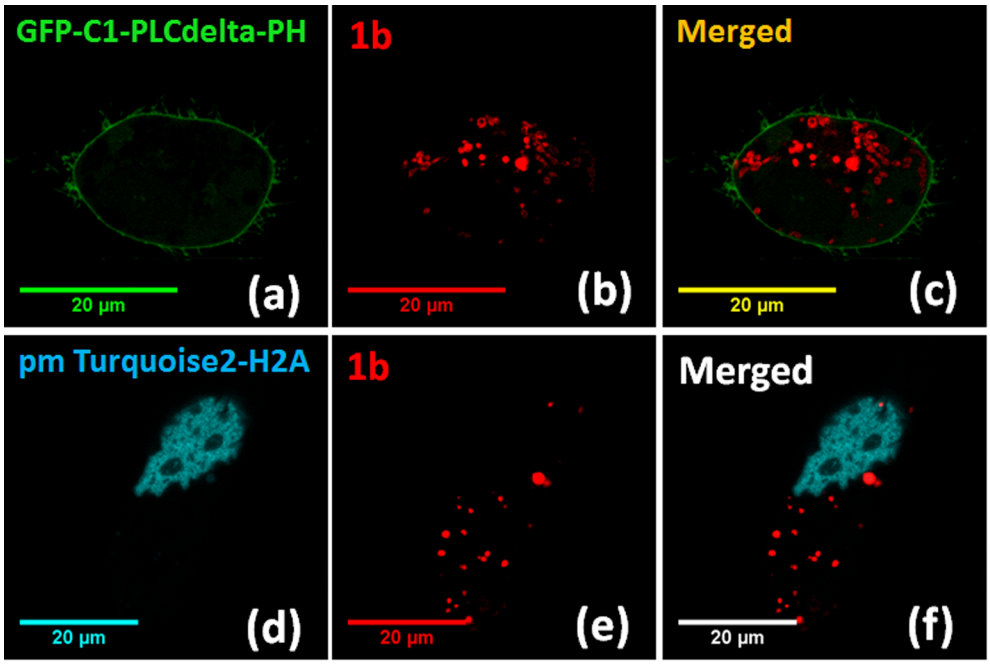

Fig. 4. Fluorescent confocal microscopy images of transfected A549 cells stained with probe **1b** (500 nM) for 30 min at 63x magnification using an oil objective. Images (a)–(c) represents GFP-C1-PLCδ-PH transfected COS-7 cells (plasma membrane) and images (d)–(f) represents Turquoise-H2A-10 transfected cells (nucleus). Images from left to right represents the confocal imaging of GFP-C1-PLCδ-PH expression (a), Turquoise-H2A-10 expression (d), Probe **1b** (b,e) and overlapped images (c,f). Probes **1b** was excited with 561 nm laser line, GFP-C1-PLCδ-PH was excited with 488 nm laser line and pm Turquoise-H2A-10 was excited with 454 nm laser line.

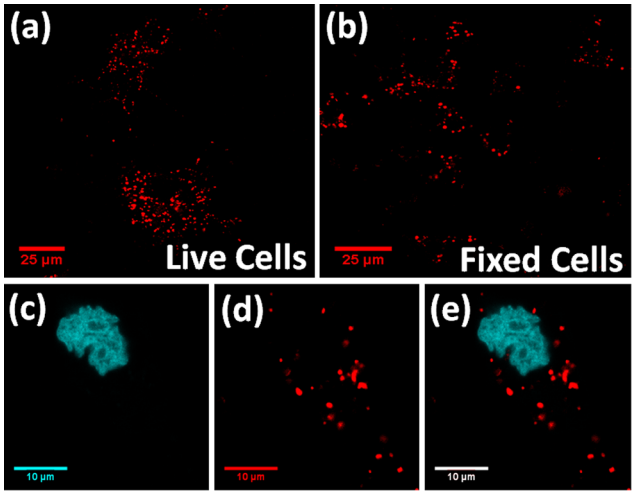

Fig. 5. (a). Fluorescence confocal microscopy images of A549 cells (live) incubated with probe **1b** (500 nM) for 30 min. (b). Fluorescence confocal microscopy images of A549 cells (fixed) incubated with probe **1b** (500 nM) for 30 min. Figures (c) to (e) represents fluorescence confocal microscopy images of mTurquoise-H2A-10 transfected A549 cells (fixed) incubated with probe **1b** (500 nM) for 30 min. Figures in the bottom row (from left to right) represents, mTurquoise-H2A-10 expression (c), probe **1b** staining (d), and composite image (e). Probe **1b** was excited with a 561 nm laser and pm Turquoise-H2A-10 was excited with 454 nm laser line. All images were obtained at 63× oil magnification.

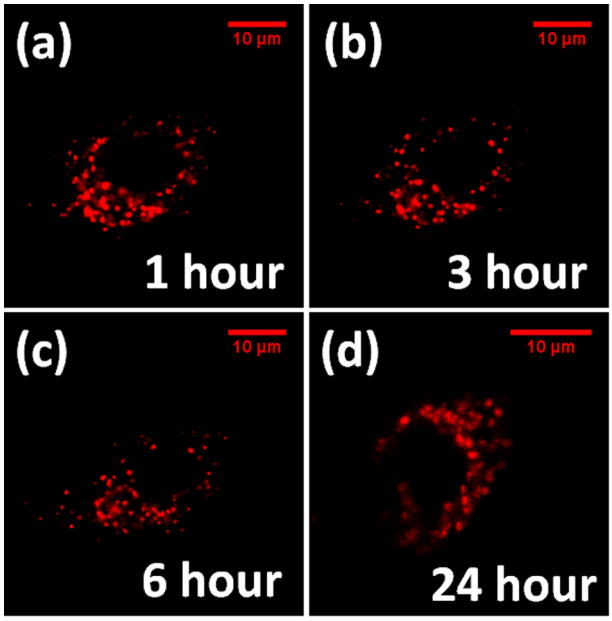

Fig. 6. Fluorescence confocal microscopy images of A549 cells incubated with **1b** (500 nM) for a 1–24 h period. Images were obtained at different time intervals including (a) 1 h, (2) 3 h, (c) 6 h, and (d) 24 h. Probe **1b** was excited with 561 nm laser line.

incubated A549 cells with commercial LysoTracker® Red DND-99 (70 nM) and cells exhibited significant changes in their morphology and staining pattern confirming potential toxic effects arising due to the characteristic alkalinizing effect (ESI Fig. S12). These results further demonstrated the suitability of new pyrene-based probes for long term imaging experiments in biological cell studies.

3.5. Probe internalization and possible interactions

Since probe **1** structure does not include a basic amino group, the intriguing question is where probe **1** would be accumulated in cellular lysosomes. It is also important to notice that absorbance or emission responses of **1** did not show any significant sensitivity towards pH. Therefore, the mechanism of interaction of probe **1** in cellular lysosomes is significantly different in comparison with acidotropic LysoTracker® probes. Also, these probes did not show any localization in plasma membrane, mitochondria (ESI Fig. S13) or nucleus of the cells compared to previously reported pyrene based probes (Fig. 4) [45,47]. These observations led us to hypothesize that these probes may be internalized into the intracellular environment in live cells by endocytosis and are accumulated in endosomal vesicles formed initially during the endocytosis process (Fig. 7). These endosomes eventually are trafficked and transformed into cellular lysosomes. Therefore, these probes may become highly fluorescent upon their accumulation in hydrophobic regions of the lysosomes (i.e., membranes, proteins).

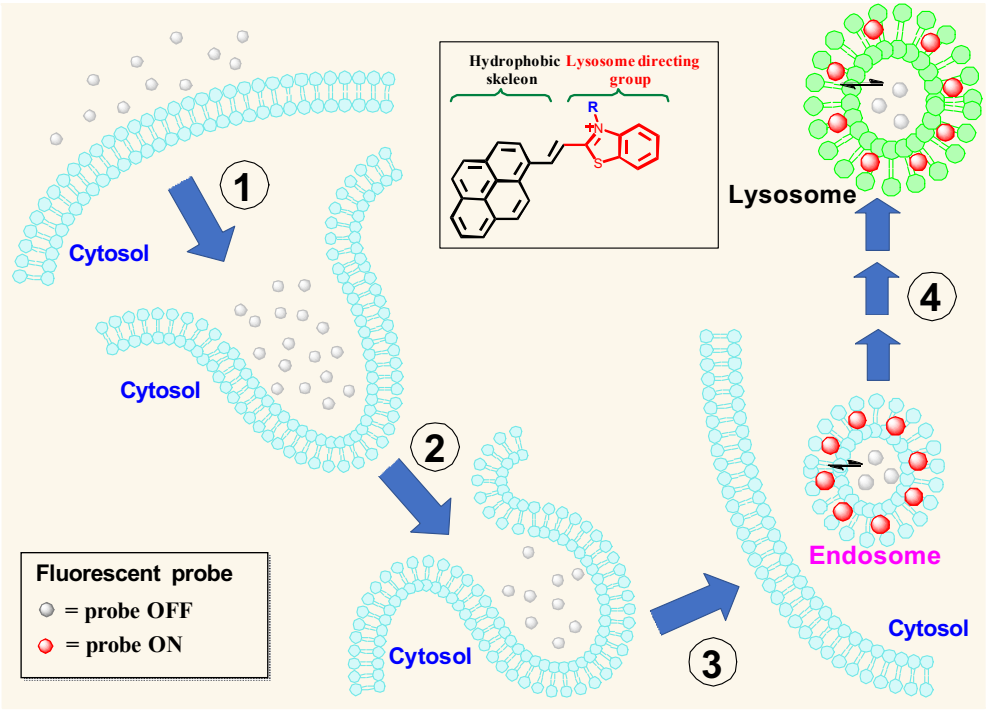

Fig. 7. Schematic representation of the possible mechanism how probes **1** localized in to cellular lysosomes via endocytosis.

Table 1
Lipophilicity calculated for probes **1a–1d**.

Probe	Log_{10} P value calculated
1a	2.07 ± 0.012
1b	2.13 ± 0.015
1c	2.17 ± 0.013
1d	2.47 ± 0.011

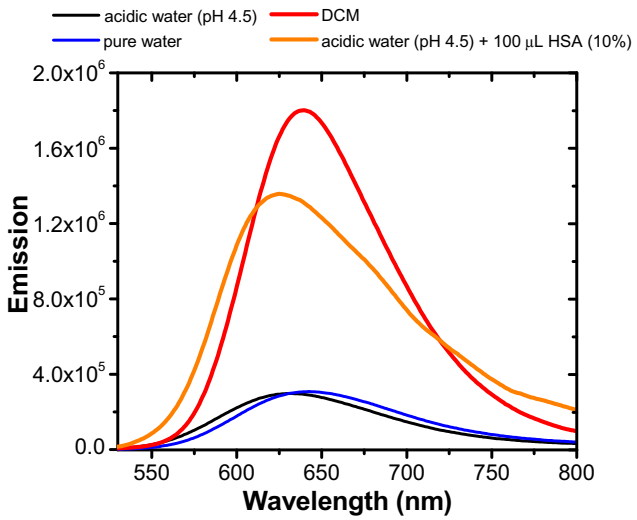

Fig. 8. Fluorescence emission of **1d** (1×10^{-5} M) in different aqueous and hydrophobic environments at room temperature.

The calculated log P values for pyrene probes were found to be in the 2.07–2.47 range, which reflected a highly lipophilic nature (Table 1). Calculated log P values further supported the hypothesis that pyrene probes **1a–1d** are more lipid soluble (lipophilic) than in aqueous environments. Therefore, it is more likely these probes may accumulate in hydrophobic (i.e., membrane) components of the cellular lysosomes.

The fluorescence emission spectra for probe **1d** was recorded in different aqueous and hydrophobic environments (Fig. 8). Interestingly, probe **1d** exhibited a significantly lower fluorescence emission in acidic (pH = 4.5) and aqueous environments compared to hydrophobic organic solvents such as methylene chloride (Fig. 8). In another experiment the addition of human serum albumin (HSA) in to an aqueous acidic (pH 4.5) solution of probe **1d** showed a large HSA-induced fluorescence turn on indicating the stabilization of the probe in hydrophobic environments (i.e., hydrophobic binding pockets) of the protein.

To further investigate possible interactions of the pyrene probes in hydrophobic lysosomal environments, probe **1d** was spectroscopically titrated and analyzed with the addition of abundant lysosomal membrane proteins (LAMP-1 and LAMP-2) in PBS buffer (pH 7.4). A solution of **1d** in PBS buffer was titrated against 5% LAMP-1 and 5% LAMP-2 protein stock solutions (in PBS buffer) and absorption - emission spectra were recorded at room temperature. Surprisingly, the addition of LAMP proteins into **1d** indicated a significant fluorescent decrease with increasing protein concentration and exhibited an aggregate formation which was evidenced as the probe out of the solution (Fig. 9a and b). Similarly, the absorption spectra of probe **1d** exhibited a sharp decrease with increasing protein concentration and showed signs of possible probe aggregation (ESI Fig. S15). Interestingly, the optical spectra of the Lysotracker® Red DND-99 did not show such response towards lysosmal membrane proteins (ESI Figs. S16–S17). The spectrometric titration result of **1d** with LAMP in aqueous acidic environments was also similar to that of aqueous buffer (ESI Figs. S18–S19). However, LysoTracker® Red DND-99 did not show any noticeable response towards LAMP proteins in acidic aqueous solutions (pH 4.5) (ESI Figs. S20–21). These results further led us to understand that these pyrene probes (**1a–1d**) may exhibit significantly different interactions in lysosome compartments compared to acidotrophic commercial LysoTracker® probes. As a control experiment probe **1d** in PBS buffer was also titrated against 5% HAS, which is a highly water-soluble transporter protein in mammals. In sharp contrast, the addition of 5% HSA into probe **1d** exhibited a significant fluorescent turn on, without showing any signs of probe aggregation from the solution (Fig. 9c and ESI Fig. S22).

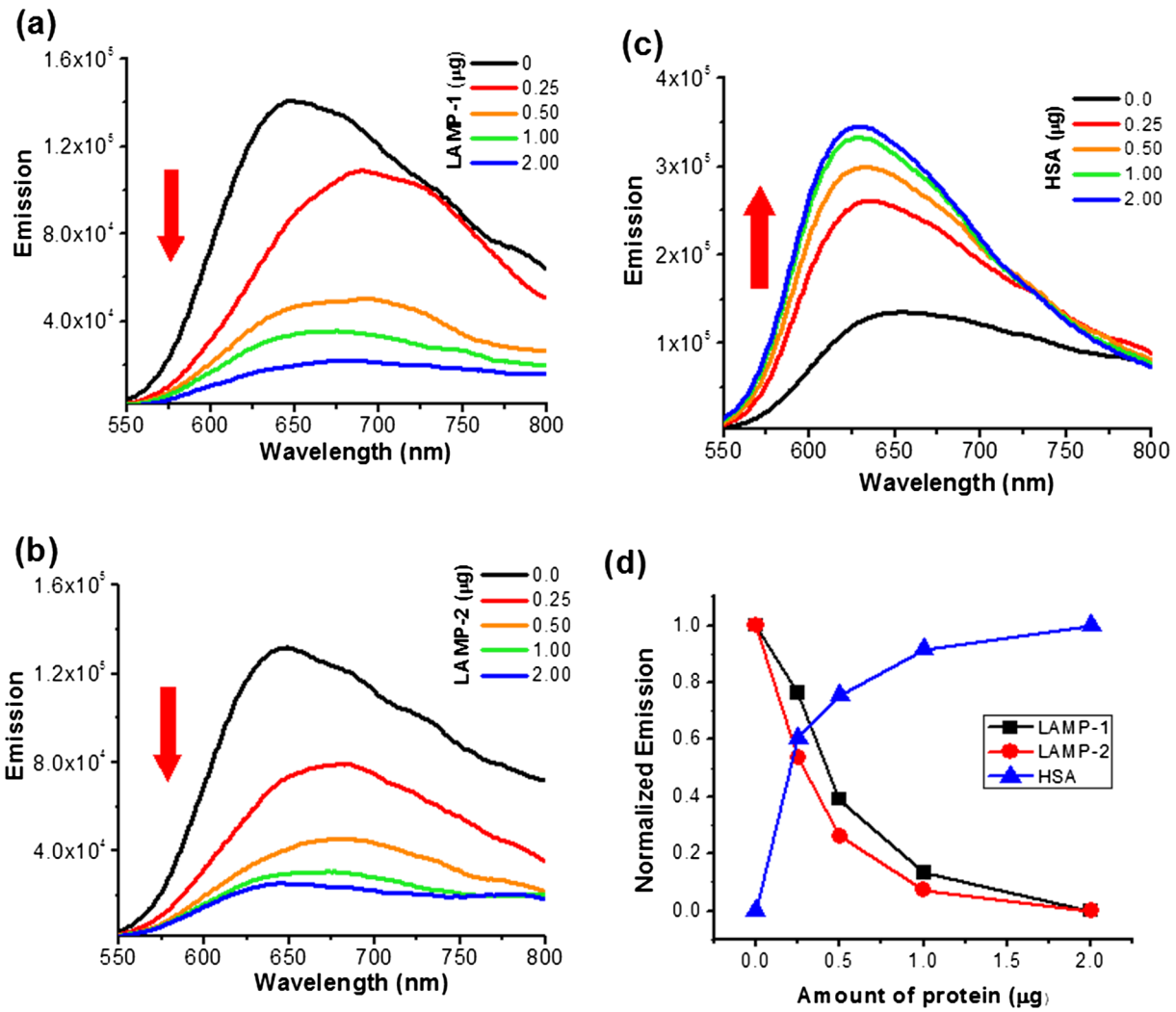

Fig. 9. Fluorescence spectra obtained for prone **1d** (1×10^{-5} M) in PBS buffer (PH 7.4) upon spectrometric titration of 5% LAMP-1 (a), 5% LAMP-2 (b), and 5% HAS (c) at room temperature. Figure (d) represents the variation of the normalized fluorescence intensity for all 3 spectrometric protein titrations. Probe **1d** was excited at 510 nm.

It is well-known that LAMP-1 and LAMP-2 are the most abundant lysosomal membrane proteins (50% >) in cellular lysosomes [27]. Therefore, the addition of highly lipophilic LAMP proteins into aqueous buffer solution of **1d** may remove the dissolved probe in the aqueous phase and deposit as aggregates along with the proteins due to strong hydrophobic interactions (possible due to the highly lipophilic nature of the pyrene probe). Therefore, the observed absorbance and emission decrease is attributed to the decreased probe concentration in the aqueous buffer solution due to aggregate formation. However, highly water-soluble proteins such as HSA could stabilize probe **1d** in their hydrophobic inner binding pockets while dispersing probe in the aqueous buffer solution without aggregating out from the solution. Therefore, the significant fluorescent enhancement observed in the presence of HSA attributing to the HSA-induced fluorescence turn on. Therefore, the above mentioned spectroscopic evidence further confirms the affinity of the pyrene probes (**1a–1d**) towards hydrophobic environments and possible accumulation in hydrophobic membrane regions of the lysosome.

In order to shed some light on understanding the internalization of the probe in to lysosomes, we decided to study the localization of probe **1b** and **1d** in COS-7 cells in the presence of endocytosis inhibitors Dyansore®[48] (Inhibitor for Clathrin mediated endocytosis) and Pitstop®2[49] (Inhibitor for Clathrin-independent endocytosis) and fluorescent confocal images were obtained (Fig. 10, ESI Fig. S10). A control experiment was carried out by incubating COS-7 cells with probes (**1b** and **1d**) in the absence of any endocytosis inhibitors. Interestingly, probes **1b** and **1d** did not show any detectable fluorescence from the lysosomes in the presence of any endocytosis inhibitors (Fig. 10, ESI Fig. S10). However, in the absence of endocytosis inhibitors bright red fluorescence from the stained lysosomes was revealed (Fig. 10). This result supported our initial hypothesis that pyrene-based probes are actively internalized into endosomes during endocytosis and may localize into hydrophobic/membrane components of the lysosome. It is well known that final destination for the molecules trafficked inside the cell via endocytosis is cellular lysosomes for breakdown/recycling. However, once internalized into lysosomes, these probes exhibited stable and consistent fluorescent emission for up to 24 h (Fig. 6). Therefore, it is possible once accumulated into cellular lysosomes, the probes are internalized and stabilized into hydrophobic regions of the lysosomes rather than staying in the acidic lysosomal lumen and undergoing breakdown by the digestive enzymes in lysosomes. It is also important to notice that probe **1** exhibits remarkably high fluorescence emission in organic/hydrophobic solvents compared to aqueous acidic solutions (pH ≈ 4.5) (Fig. 8 and ESI Fig. S11). Also, it is important to note that wash-free staining based fluorescence confocal microscopy images did not show any background fluorescence suggesting weaker/non-emissive nature of the probe in aqueous environments (ESI Fig. S14).

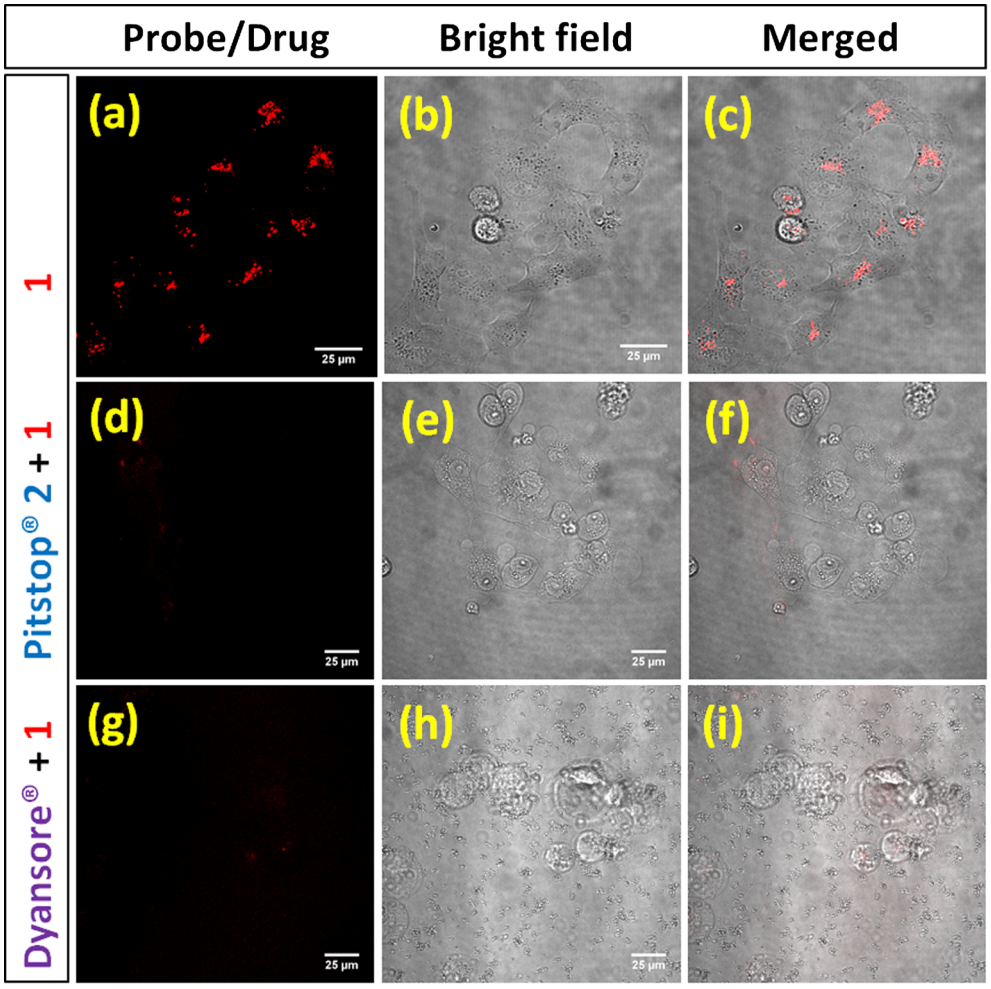

Fig. 10. Confocal microscope images obtained for COS-7 cells upon incubation with probe **1d** (500 nM) for 30 min in the absence (a–c) and presence (d–i) of the endocytosis inhibitors Pitstop® 2 (25 µM, d–f) and Dyansore® (80 µM, g–i). Probe **1d** was excited with a 561 nm laser. The scale bar is 25 µm.

Therefore, accumulation of these probes into the lysosomal lumen may not likely turn on fluorescence. It should be noted that LysoTracker® probes are accumulated in lysosomes via simple diffusion and known to generate emission from the lysosome lumen [50,51], while LAMP-1 expression-based transfection imaging is originating from the lysosomal membranes. It is also important to note that the pyrene-based probe with a pyridinium moiety will be localized in the cell nucleus, as our previous research shows [45]. Also, previous work reported pyerene-imidazolium probes as excellent mitochondria probes [52]. Therefore, the benzothiazolium moiety in this probe structure considered as the key component for observed lysosome selective labeling ability of probe **1** [42]. However, the attachment of pyrene skeleton has given the advantage for probes to be stabilized into hydrophobic components of the lysosome and produced bright red fluorescence. Probe **1** also did not show any significant absorption or emission response towards pH changes (pH = 3–8) in the media (ESI Fig. S2.2), as both pyrene and benzothiazolium segments are quite inert to protonation. Therefore, the acidic environment in the lysosome may not likely to promote accumulation of **1** in the lysosome lumen. Therefore, this new pyrene-based probe series would be an outstanding tool for visualizing cellular lysosomes in both healthy and cancer cell lines for long term experiments without perturbing cellular activities.

4. Conclusions

In conclusion, a highly biocompatible series of fluorescent probes have been successfully developed for lysosome detection in live cells without any alkalinizing effects. These probes exhibited a stable emission throughout a wide pH range (1.0–12.0), as the probe structure is insensitive to acidity. Probes exhibited remarkable selectivity for visualizing lysosomes in both healthy and tumor cells. Currently, many studies rely on lysosome-associated membrane protein-1 (LAMP-1) to detect lysosomes, which uses fluorescently tagged lysosome specific proteins to label lysosome membranes. The new pyrene-based probes are found to exhibit improved lysosome selectivity, in comparison with LAMP-1 expression-based lysosome visualization that often gives significant background fluorescence in cancer cells, due to non-selective expression of LAMP-1. Probes exhibited an ability to visualize lysosomes in both live cells and fixed cells for imaging experiments. The entry and accumulation of the probes in lysosomes of live cells was found to be dependent on endocytosis whereas the ability of the probes to access and label lysosomes of fixed cells is still unknown. In addition, these new pyrene-based probes will be powerful tools due to their ability to visualize cellular lysosomes for long-term imaging experiments. Therefore, these new probes could be valuable tools for monitoring lysosome activities and in cancer research, as they likely exert minimal perturbation on the digestive activities of lysosomal enzymes.

Acknowledgment

K.J.W. was supported by a NIH CBBI fellowship (T32GM075762). The imaging studies were supported by the Indiana University School of Medicine-South Bend Imaging and Flow Cytometry core (to R.V.S.). We also thank Dr. Charles Tessier from the Indiana University School of

Medicine-South Bend Imaging and Flow Cytometry core, for support.

Contributions

C. S. A. planned, conducted, and summarized the synthesis of probes. K. J. W. and C. S. A. planned and performed cell experiments. R. V. S. and Y. P. designed and supervised the project. C. S. A., K. J. W., R.V.S., and Y. P. wrote the manuscript.

Declaration of Competing Interest

Authors declare no competing interests.

Appendix A. Supplementary material

Supplementary data to this article can be found online at https://doi.org/10.1016/j.bioorg.2019.103144.

References

[1] N.B. Yapici, Y. Bi, P. Li, X. Chen, X. Yan, S.R. Mandalapu, M. Faucett, S. Jockusch, J. Ju, K.M. Gibson, Highly stable and sensitive fluorescent probes (LysoProbes) for lysosomal labeling and tracking, Sci. Rep. 5 (2015) 1–8.
[2] E.J. Parkinson-Lawrence, T. Shandala, M. Prodoehl, R. Plew, G.N. Borlace, D.A. Brooks, Lysosomal storage disease: revealing lysosomal function and physiology, Physiology 25 (2010) 102–115.
[3] T. Kirkegaard, M. Jäättelä, Lysosomal involvement in cell death and cancer, Biochim. Biophys. Acta - Mol. Cell Res. 1793 (2009) 746–754.
[4] H. Maes, P. Agostinis, Autophagy and mitophagy interplay in melanoma progression, Mitochondrion (2014) 58–68.
[5] P. Honscheid, K. Datta, M.H. Muders, Autophagy: detection, regulation and its role in cancer and therapy response, Int. J. Radiat. Biol. 90 (2014) 628–635.
[6] P. Jiang, N. Mizushima, Autophagy and human diseases, Cell Res. 24 (2014) 69–79.
[7] X. He, J. Li, S. An, C. Jiang, pH-sensitive drug-delivery systems for tumor targeting, Ther. Deliv. 4 (2013) 1499–1510.
[8] J. Reyjal, K. Cormier, S. Turcotte, Autophagy and cell death to target cancer cells: exploiting synthetic lethality as cancer therapies, Adv. Exp. Med. Biol. 2014, pp. 167–188.
[9] R. Ashoor, R. Yafawi, B. Jessen, S. Lu, The contribution of lysosomotropism to autophagy perturbation, PLoS One 8 (2013).
[10] F.M. Platt, Emptying the stores: lysosomal diseases and therapeutic strategies, Nat. Rev. Drug Discov. 17 (2018) 133.
[11] M.M. Mohamed, B.F. Sloane, Cysteine cathepsins: multifunctional enzymes in cancer, Nat. Rev. Cancer (2006) 764–775.
[12] S.S. Jensen, C. Aaberg-Jessen, K.G. Christensen, B. Kristensen, Expression of the lysosomal-associated membrane protein-1 (LAMP-1) in astrocytomas, Int. J. Clin. Exp. Pathol. 6 (2013) 1294–1305.
[13] T. Reinheckel, J. Deussing, W. Roth, C. Peters, Towards specific functions of lysosomal cysteine peptidases: phenotypes of mice deficient for cathepsin B or cathepsin L, Biol. Chem. 382 (2001) 735–741.
[14] K.N. Balaji, N. Schaschke, W. Machleidt, M. Catalfamo, P.A. Henkart, Surface cathepsin B protects cytotoxic lymphocytes from self-destruction after degranulation, J. Exp. Med. 196 (2002) 493–503.
[15] U. Felbor, B. Kessler, W. Mothes, H.H. Goebel, H.L. Ploegh, R.T. Bronson, B.R. Olsen, Neuronal loss and brain atrophy in mice lacking cathepsins B and L, Proc. Natl. Acad. Sci. USA 99 (2002) 7883–7888.
[16] M.E. Guicciardi, M. Leist, G.J. Gores, Lysosomes in cell death, Oncogene 23 (2004) 2881–2890.
[17] M. Jaattela, Multiple cell death pathways as regulators of tumour initiation and progression, Oncogene 23 (2004) 2746–2756.
[18] S. Piao, R.K. Amaravadi, Targeting the lysosome in cancer, Ann. N. Y. Acad. Sci. 1371 (2016) 45–54.
[19] U. Repnik, V. Stoka, V. Turk, B. Turk, Lysosomes and lysosomal cathepsins in cell death, Biochim. Biophys. Acta - Proteins Proteom. 2012 (1824) 22–33.
[20] N.P. Withana, G. Blum, M. Sameni, C. Slaney, A. Anbalagan, M.B. Olive, B.N. Bidwell, L. Edgington, L. Wang, K. Moin, B.F. Sloane, R.L. Anderson, M.S. Bogyo, B.S. Parker, Cathepsin B inhibition limits bone metastasis in breast cancer, Cancer Res. 72 (2012) 1199–1209.
[21] P. Saftig, B. Schröder, J. Blanz, Lysosomal membrane proteins: life between acid and neutral conditions, Biochem. Soc. Trans. 38 (2010) 1420–1423.
[22] P. Saftig, J. Klumperman, Lysosome biogenesis and lysosomal membrane proteins: trafficking meets function, Nat. Rev. Mol. Cell Biol. 10 (2009) 623–635.
[23] L. Groth-Pedersen, M. Jäättelä, Combating apoptosis and multidrug resistant cancers by targeting lysosomes, Cancer Lett. 332 (2013) 265–274.
[24] M. Schwake, B. Schröder, P. Saftig, Lysosomal membrane proteins and their central role in physiology, Traffic 14 (2013) 739–748.
[25] E.J. Parkinson-Lawrence, C.J. Dean, M. Chang, J.J. Hopwood, P.J. Meikle, D.A. Brooks, Immunochemical analysis of CD107a (LAMP-1), Cell. Immunol. (2005) 161–166.
[26] K. Furuta, M. Ikeda, Y. Nakayama, K. Nakamura, M. Tanaka, N. Hamasaki, M. Himeno, S.R. Hamilton, J.T. August, Expression of lysosome-associated membrane proteins in human colorectal neoplasms and inflammatory diseases, Am. J. Pathol. 159 (2001) 449–455.
[27] B.M. Künzli, P.O. Berberat, Z.W. Zhu, M. Martignoni, J. Kleeff, A.A. Tempia-Caliera, M. Fukuda, A. Zimmermann, H. Friess, M.W. Büchler, Influences of the lysosomal associated membrane proteins (Lamp-1, Lamp-2) and Mac-2 binding protein (Mac-2-BP) on the prognosis of pancreatic carcinoma, Cancer 94 (2002) 228–239.
[28] N. Andrejewski, E.L. Punnonen, G. Guhde, Y. Tanaka, R. Lüllmann-Rauch, D. Hartmann, K. Von Figura, P. Saftig, Normal lysosomal morphology and function in LAMP-1-deficient mice, J. Biol. Chem. 274 (1999) 12692–12701.
[29] R.P. Haugland, The Handbook: A Guide to Fluorescent Probes and Labeling Technologies, Molecular probes, 2005.
[30] G.Y. Wiederschain, The Molecular Probes handbook. A guide to fluorescent probes and labeling technologies, Biochemistry 76 (2011) 1276.
[31] X. Zhang, C. Wang, Z. Han, Y. Xiao, A photostable near-infrared fluorescent tracker with pH-independent specificity to lysosomes for long time and multicolor imaging, ACS Appl. Mater. Interfaces. 6 (2014) 21669–21676.
[32] H. Zhu, J. Fan, Q. Xu, H. Li, J. Wang, P. Gao, X. Peng, Imaging of lysosomal pH changes with a fluorescent sensor containing a novel lysosome-locating group, Chem. Commun. 48 (2012) 11766–11768.
[33] H.M. Kim, M.J. An, J.H. Hong, B.H. Jeong, O. Kwon, J.Y. Hyon, S.C. Hong, K.J. Lee, B.R. Cho, Two-photon fluorescent probes for acidic vesicles in live cells and tissue, Angew. Chem. - Int. Ed. 47 (2008) 2231–2234.
[34] B. Wang, S. Yu, X. Chai, T. Li, Q. Wu, T. Wang, A lysosome-compatible near-infrared fluorescent probe for targeted monitoring of nitric oxide, Chem. - A Eur. J. 22 (2016) 5649–5656.
[35] Y. Han, M. Li, F. Qiu, M. Zhang, Y.-H. Zhang, Cell-permeable organic fluorescent probes for live-cell long-term super-resolution imaging reveal lysosome-mitochondrion interactions, Nat. Commun. 8 (2017) 1307.
[36] D. Dahal, L. McDonald, X. Bi, C. Abeywickrama, F. Gombedza, M. Konopka, S. Paruchuri, Y. Pang, An NIR-emitting lysosome-targeting probe with large Stokes shift via coupling cyanine and excited-state intramolecular proton transfer, Chem. Commun. 53 (2017) 3697–3700.
[37] C. Duan, J.-F. Zhang, Y. Hu, L. Zeng, D. Su, G.-M. Bao, A distinctive near-infrared fluorescence turn-on probe for rapid, sensitive and chromogenic detection of sulfite in food, Dye. Pigm. 162 (2019) 459–465.
[38] C. Duan, M. Won, P. Verwilst, J. Xu, H.S. Kim, L. Zeng, J.S. Kim, In vivo imaging of endogenously produced HClO in zebrafish and mice using a bright, photostable ratiometric fluorescent probe, Anal. Chem. (2019), https://doi.org/10.1021/acs.analchem.9b00224.
[39] A. Pierzyńska-Mach, P.A. Janowski, J.W. Dobrucki, Evaluation of acridine orange, LysoTracker Red, and quinacrine as fluorescent probes for long-term tracking of acidic vesicles, Cytom. Part A 85 (2014) 729–737.
[40] T. Myochin, K. Kiyose, K. Hanaoka, H. Kojima, T. Terai, T. Nagano, Rational design of ratiometric near-infrared fluorescent pH probes with various pKa values, based on aminocyanine, J. Am. Chem. Soc. 133 (2011) 3401–3409.
[41] D.G. Smith, B.K. McMahon, R. Pal, D. Parker, Live cell imaging of lysosomal pH changes with pH responsive ratiometric lanthanide probes, Chem. Commun. 48 (2012) 8520.
[42] C.S. Abeywickrama, K.J. Wijesinghe, R.V. Stahelin, Y. Pang, Red-emitting pyrene-benzothiazolium: unexpected selectivity to lysosomes for real-time cell imaging without alkalinizing effect, Chem. Commun. (Camb.) 55 (2019) 3469–3472.
[43] A. Leo, P.Y.C. Jow, C. Silipo, C. Hansch, Calculation of hydrophobic constant (log P) from. pi. and f constants, J. Med. Chem. 18 (1975) 865–868, https://doi.org/10.1021/jm00243a001.
[44] R. Mannhold, G.I. Poda, C. Ostermann, I.V. Tetko, Calculation of molecular lipophilicity: state-of-the-art and comparison of log P methods on more than 96,000 compounds, J. Pharm. Sci. 98 (2009) 861–893, https://doi.org/10.1002/jps.21494.
[45] C.S. Abeywickrama, K.J. Wijesinghe, R.V. Stahelin, Y. Pang, Bright red-emitting pyrene derivatives with a large Stokes shift for nucleus staining, Chem. Commun. 53 (2017) 5886–5889, https://doi.org/10.1039/C7CC03417B.
[46] J. Goedhart, D. Von Stetten, M. Noirclerc-Savoye, M. Lelimousin, L. Joosen, M.A. Hink, L. Van Weeren, T.W.J. Gadella, A. Royant, Structure-guided evolution of cyan fluorescent proteins towards a quantum yield of 93%, Nat. Commun. 3 (2012), https://doi.org/10.1038/ncomms1738.
[47] Y. Niko, P. Didier, Y. Mely, G.I. Konishi, A.S. Klymchenko, Bright and photostable push-pull pyrene dye visualizes lipid order variation between plasma and intracellular membranes, Sci. Rep. 6 (2016), https://doi.org/10.1038/srep18870.
[48] T. Kirchhausen, E. Macia, H.E. Pelish, Use of dynasore, the small molecule inhibitor of dynamin, in the regulation of endocytosis, Meth. Enzymol. 438 (2008) 77–93.
[49] D. Dutta, C.D. Williamson, N.B. Cole, J.G. Donaldson, Pitstop 2 is a potent inhibitor of clathrin-independent endocytosis, PLoS One 7 (2012).
[50] B. Zhitomirsky, H. Farber, Y.G. Assaraf, LysoTracker and MitoTracker Red are transport substrates of P-glycoprotein: implications for anticancer drug design evading multidrug resistance, J. Cell. Mol. Med. 22 (2018) 2131–2141.
[51] M. Duvvuri, Y. Gong, D. Chatterji, J.P. Krise, Weak base permeability characteristics influence the intracellular sequestration site in the multidrug-resistant human leukemic cell line HL-60, J. Biol. Chem. 279 (2004) 32367–32372.
[52] Q. Hu, C. Qin, L. Huang, H. Wang, Q. Liu, L. Zeng, Selective visualization of hypochlorite and its fluctuation in cancer cells by a mitochondria-targeting ratiometric fluorescent probe, Dye. Pigm. 149 (2018) 253–260.